

Live Fast, Die Young: GMC lifetimes in the FIRE cosmological simulations of Milky Way-mass galaxies

Samantha M. Benincasa,¹★ Sarah R. Loebman,¹† Andrew Wetzel,¹ Philip F. Hopkins,² Norman Murray,^{3,4} Matthew A. Bellardini,¹ Claude-André Faucher-Giguère,⁵ Dávid Guszejnov,⁶ and Matthew Orr²

¹Department of Physics, University of California, Davis, CA 95616, USA

²TAPIR, Mailcode 350-17, California Institute of Technology, Pasadena, CA, 91125

³Canadian Institute for Theoretical Astrophysics, 60 St. George Street, University of Toronto, ON M5S 3H8, Canada

⁴Canada Research Chair in Astrophysics

⁵Department of Physics and Astronomy and Center for Interdisciplinary Exploration and Research in Astrophysics (CIERA), Northwestern University, 2145 Sheridan Road, Evanston, IL 60208, USA

Accepted XXX. Received YYY; in original form ZZZ

ABSTRACT

We present the first measurement of the lifetimes of Giant Molecular Clouds (GMCs) in cosmological simulations at $z = 0$, using the Latte suite of FIRE-2 simulations of Milky Way-mass galaxies. We track GMCs with total gas mass $\gtrsim 10^5 \text{ M}_\odot$ at high spatial ($\sim 1 \text{ pc}$), mass (7100 M_\odot), and temporal (1 Myr) resolution. Our simulated GMCs are consistent with the distribution of masses for massive GMCs in the Milky Way and nearby galaxies. We find GMC lifetimes of 5–7 Myr, or 1–2 freefall times, on average, with less than 1% of clouds living longer than 20 Myr. We find increasing GMC lifetimes with galactocentric radius, implying that environment affects the evolutionary cycle of GMCs. However, our GMC lifetimes show no systematic dependence on GMC mass or amount of star formation. These results are broadly consistent with inferences from the literature and provide an initial investigation into ultimately understanding the physical processes that govern GMC lifetimes in a cosmological setting.

Key words: galaxies: ISM – ISM: clouds – ISM: evolution

1 INTRODUCTION

As the birthplace of stars, GMCs are fundamental to our understanding of star formation and the baryon life cycle. Because we are entering an era of high-precision measurements of dense gas in the Milky Way (MW) and nearby galaxies, we are newly positioned to make great strides in our understanding of the physics governing GMCs (e.g. Schinnerer et al. 2019).

The galactic environment, including the dynamical state of the ISM, affects the properties of GMCs: there is no universal set of cloud properties across all galaxies. For example, Sun et al. (2018) find that, for GMCs with a small range in virial parameters, different galactic environments can drive wildly different internal states, such as turbulent pressure. Furthermore, understanding pressure confinement

in the ISM may be important to understanding the internal states of GMCs (e.g. Faesi et al. 2018; Schruba et al. 2019).

We only now are beginning to understand the connections between star formation and the life cycle of GMCs. Constraining the lifetimes of GMCs is critical to constraining the physics of the cycle of star formation, including how dense gas cycles through the ISM. The amount of time gas spends in the star-forming state can explain the long depletion time in galaxies (Semenov et al. 2017), although larger-scale galactic equilibria ultimately may determine the low efficiency of galactic star formation (e.g. Ostriker et al. 2010). In principle, GMC lifetimes are sensitive to the form(s) of stellar feedback that are most critical to truncating star formation (e.g. Lopez et al. 2014; Howard et al. 2017; Kruijssen et al. 2019).

Recent work, both theoretical and observational, has shed light on the lifetimes of GMCs. Observational measurements of lifetimes require a statistical approach, because we cannot track GMCs in real time. Miura et al. (2012) use the

★ E-mail: smbenincasa@ucdavis.edu

† Hubble Fellow

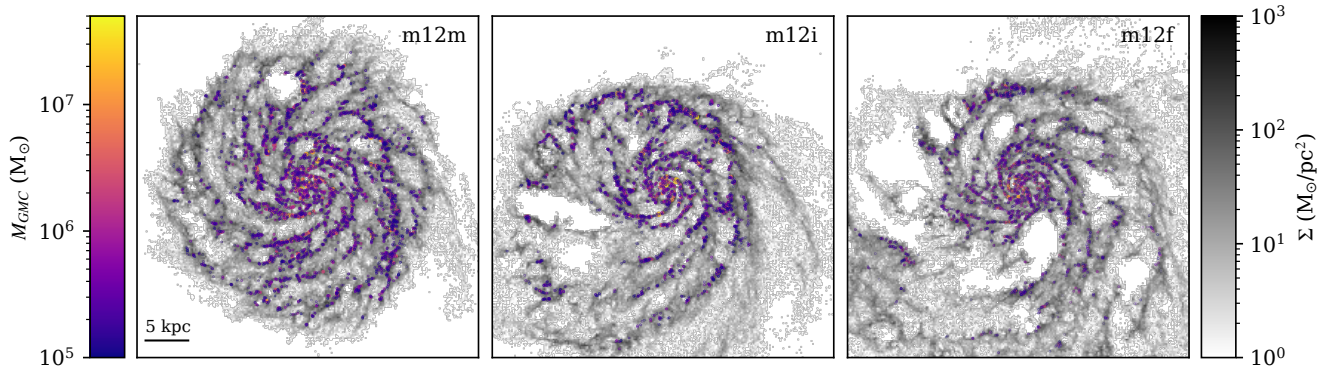


Figure 1. Maps of gas surface density at $z = 0$ for the 3 cosmological zoom-in simulations in this work. We show the cold gas surface density via the greyscale map in the background. We overlay the locations of GMCs, coloured by their mass. Each image is 40 kpc across. At a given time, we identify ~ 1200 GMCs in **m12i**, ~ 2700 GMCs in **m12m** and ~ 1600 GMCs in **m12f** with $M \gtrsim 10^5 M_\odot$.

connection between the evolutionary states of GMCs and young stellar objects to infer lifetimes in M33 of 20 – 40 Myr. Another approach is to compare the spatial distributions of gas tracer peaks and stellar tracer peaks (Kruijssen & Longmore 2014; Kruijssen et al. 2018). Kruijssen et al. (2019) infer lifetimes of ~ 10 Myr in NGC 300, based on the lifetime of the CO emitting gas in the clouds. In the MW, Murray (2011) estimate lifetimes of massive GMCs of 27 ± 12 Myr. However, these are indirect inferences of GMC lifetimes.

A large catalog of theoretical work now complements these observational studies. Analytical calculations favour GMC lifetimes of a few crossing/dynamical times (e.g. Krumholz et al. 2006; Elmegreen 2007). Recently, Jefferson & Kruijssen (2018) have built upon this work, comparing important physical timescales impacting GMC evolution, leading to an estimated GMC lifetime of 10 – 50 Myr. Furthermore, various works have used isolated (non-cosmological) simulations to achieve the necessary high dynamic range across a full galactic disk to disentangle environmental dependence (e.g. Ward et al. 2016; Grisdale et al. 2018; Pettitt et al. 2018; Dobbs et al. 2019). Here, one can track the evolution of single cloud or cloud complex. Highly resolved studies of individual GMCs have found lifetimes of typically ~ 1 – 2 freefall times (e.g. Harper-Clark & Murray 2011; Grudić et al. 2018). However, these works do not capture the galactic environment, global evolution, confinement from the surrounding ISM nor accretion. In isolated (non-cosmological) galaxy simulations, one can measure GMC lifetimes by tracking mass gain and loss of a full population of GMCs over time (Hopkins et al. 2012; Dobbs & Pringle 2013; Grisdale et al. 2019). For example, Dobbs & Pringle (2013) find cloud lifetimes of 4 – 25 Myr in isolated (non-cosmological) galaxy simulations with imposed spiral potentials. Similarly, Hopkins et al. (2012) find cloud lifetimes with a median of 4 – 5 Myr.

Cosmological galaxy simulations now offer new laboratories for examining GMC properties and lifetimes directly in galactic environments in cosmological settings. Suites of cosmological zoom-in simulations now offer sufficient dynamic range across a range of galactic morphologies and properties, including larger-scale processes like cosmic gas accretion, wind recycling, and perturbations from satellite

galaxies. These are important sources for driving turbulence in the interstellar medium (ISM).

In this Letter, we present the first measurement of GMC lifetimes in cosmological zoom-in simulations of MW/M31-mass galaxies at $z = 0$, examining dependence on galactic environment, GMC mass, and GMC star-formation activity.

2 METHODS

We analyze 3 galaxies from the Latte suite of FIRE-2 cosmological zoom-in simulations of MW/M31-mass galaxies (Wetzel et al. 2016). We ran these simulations using the FIRE-2 physics model (Hopkins et al. 2018), employing the Lagrangian meshless finite-mass hydrodynamics code GIZMO (Hopkins 2015). These simulations explicitly model stellar feedback from core-collapse and type Ia supernovae, stellar winds, photoionization, photoelectric heating and radiation pressure, as detailed in Hopkins et al. (2018), including gas heating and cooling across 10 – 10^{10} K. Star formation occurs in gas that is self-gravitating, Jeans-unstable, cold ($T < 10^4$ K), dense ($n > 1000 \text{ cm}^{-3}$), and molecular (following Krumholz & Gnedin 2011). These simulation have gas and (initial) star particle masses of $7100 M_\odot$. Gas hydrodynamic smoothing is fully adaptive and is identical to force softening, reaching a minimum of 1 pc (Plummer equivalent), with force softening in the typical ISM (densities $\sim 1 \text{ cm}^{-3}$) of ~ 20 pc. The force softening of star and dark-matter particles is 4 and 40 pc.

We focus on 3 galaxies that are particularly MW/M31-like in mass and size: **m12i**, **m12m**, and **m12f** (Wetzel et al. 2016; Hopkins et al. 2018; Sanderson et al. 2018). These span a range in morphology: **m12m** is a flocculent spiral while **m12f** has had a recent interaction resulting in a slightly disturbed morphology. The total stellar masses for **m12m**, **m12i** and **m12f** are $7.9 \times 10^{10} M_\odot$, $6.3 \times 10^{10} M_\odot$ and $5.1 \times 10^{10} M_\odot$, respectively. The total gas masses for **m12m**, **m12i** and **m12f** are $2.1 \times 10^{10} M_\odot$, $1.6 \times 10^{10} M_\odot$ and $2.3 \times 10^{10} M_\odot$, respectively as measured within R_{90} . For comparison, as measured within the virial radius, the total baryonic mass of the MW is $8.5 \pm 1.3 \times 10^{10} M_\odot$, with $5.1 \times 10^{10} M_\odot$ in stars (Bland-Hawthorn & Gerhard 2016). For this work, we re-simulated these 3 galaxies to store snapshots every 1 Myr over the final 100 Myr before $z = 0$. Figure 1 shows gas surface density maps for these 3 galaxies at $z = 0$. Several works have examined the ISM properties of these simulated galax-

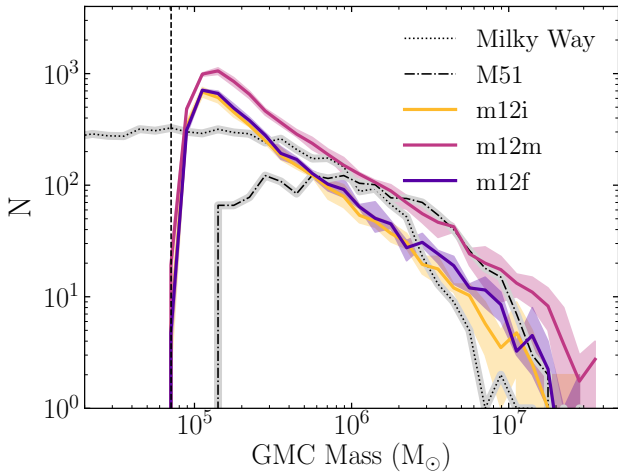


Figure 2. The distribution of GMC masses in our 3 cosmological simulations at $z \approx 0$. The shaded region shows the range across different snapshots. We compare to observed GMCs in the Milky Way (Miville-Deschénes et al. 2017) and M51 (Colombo et al. 2014). Our simulated GMC mass distributions are broadly within the ranges of those observed, though we note an apparent excess at low mass, near our resolution limit (20 gas elements).

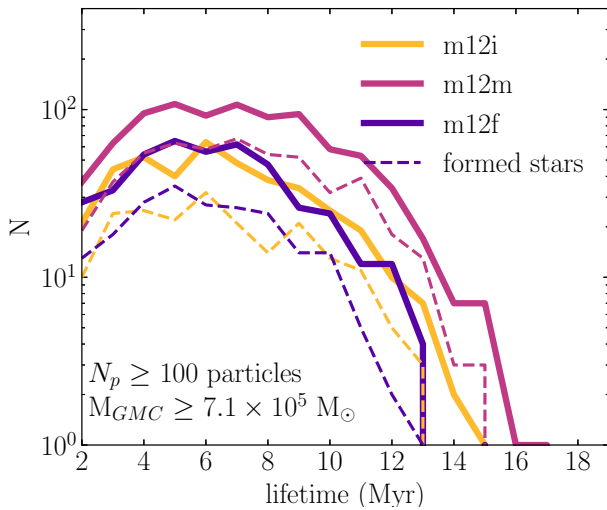


Figure 3. The distribution of GMC lifetimes in each of our 3 cosmological simulations at $z \approx 0$, for clouds with at least 100 resolution elements. The mean lifetime is ~ 6 Myr, with less than 1% of clouds living longer than 20 Myr. Dashed curves show clouds that hosted any level of star formation; we do not find significant differences based on star-formation activity. These lifetimes are broadly consistent with both observational and theoretical work (typically 10 – 20 Myr); though our average favours shorter lifetimes, in the massive GMCs that we resolve.

ies (Sanderson et al. 2018; Orr et al. 2018; El-Badry et al. 2018b,a; Hung et al. 2019; Guszejnov et al. 2019).

2.1 Identifying Clouds

We identify GMCs using a Friends-of-Friends (FoF) algorithm, which groups gas elements based on proximity via an isodensity threshold. FoF requires a single free parameter, the linking length, l , which determines the isodensity threshold. After extensive testing, we choose a linking length

of 20 pc for identifying GMCs, which corresponds to a local density of ~ 30 cm $^{-3}$. Additionally, we consider only gas elements with hydrodynamic kernel densities > 10 cm $^{-3}$ and with temperatures below 10 4 K. We confirmed that these cuts have no impact on the identified GMCs, but they significantly increase the speed of finding. This method is consistent with that of Lakhani et al. (in prep). Figure 1 shows the locations of these GMCs, overlaid on the maps of total gas surface density. We analyze GMCs with more than 20 gas elements, corresponding to a minimum mass of $\sim 10^5$ M $_{\odot}$. Thus, by GMC ‘mass’ we mean the sum of the masses of all gas elements in the cloud.

Figure 2 shows the properties of GMCs in our simulations at $z = 0$, compared with GMCs observed in both the MW and M51. For comparison, M51 has a stellar mass of 3.6×10^{10} M $_{\odot}$ and a gas fraction of 0.2 (Shetty et al. 2007; Leroy et al. 2008; Schinnerer et al. 2013). The MW has a stellar mass of 6×10^{10} M $_{\odot}$ (Licquia & Newman 2015). The top panel shows the mass distribution of GMCs in our simulated galaxies compared to GMCs in M51 (dot-dashed line) and the MW (dotted line). We use the M51 sample from Colombo et al. (2014) and the MW sample from Miville-Deschénes et al. (2017). The rollover of the GMC mass distribution for M51 shows the position of the adopted completeness limit of 3.6×10^5 M $_{\odot}$ (Colombo et al. 2014). In contrast, studies of the MW are complete down to lower masses (Miville-Deschénes et al. 2017; Roman-Duval et al. 2010). The vertical dashed line shows our resolution limit, which matches closely the completeness limit for M51. From this comparison it appears that our simulations produce a possible excess of GMCs approaching the mass resolution limit. **However, the shape of the mass function at the resolution limit is particularly sensitive to the GMC identification algorithm.** Further, while we currently probe only the massive GMCs in our simulations, in future work we will resolve an order of magnitude lower cloud mass.

2.2 Tracking the Evolution of Clouds

To track the evolution of clouds, we follow the methodology used in previous studies (e.g. Hopkins et al. 2012; Dobbs & Pringle 2013). Given a specific GMC i in snapshot n , we identify the descendant or progenitor of this GMC (in snapshot $n \pm 1$) as the FOF group that contains the most total mass in elements from the original GMC i . We take the reference GMC at arbitrary snapshots, spaced by 10 Myr to avoid double counting. We track each cloud forward and backward until it has lost 50% of its original/reference mass. We also stop tracking if the cloud’s elements no longer make up the main constituent after a merger, for example, when a cloud is absorbed into a larger cloud. In this Letter, we examine only the subset of clouds that die according to the mass loss criterion; we will examine clouds that die via agglomeration into a larger cloud in future work. This agglomerated subset constitutes $\sim 65\%$ of all clouds, and $\sim 58\%$ of clouds in our population of most massive clouds, with $N_p > 100$.

Of course, the choice of mass threshold impacts the resultant lifetime measurement. We tested this by examining lifetimes using mass cutoffs of $1/2$, $1/e$, and $1/5$ of the original mass. These lead to small changes to the peak of the GMC lifetime distribution, increasing it by 1–2 Myr. We also

Table 1. Mean and standard deviation of GMC lifetimes across our 3 cosmological simulations, for all GMCs, and those that form stars. N_p indicates the minimum number of gas elements, effectively a mass threshold.

	all GMCs			formed stars	
	N_p	$\langle l \rangle$ (Myr)	σ (Myr)	$\langle l \rangle$ (Myr)	σ (Myr)
m12i	20	6.16	3.14	6.08	2.92
	100	6.48	2.8	6.47	2.82
m12m	20	6.01	3.13	6.29	3.11
	100	7.03	2.96	7.08	2.92
m12f	20	5.86	3.04	5.96	2.96
	100	6.27	2.6	6.09	2.44

measure lifetimes of the overdense gas cloud as a coherent unit; we do not follow the creation or destruction of molecular gas, so are *not* measuring the lifetimes of molecules or other species within clouds. One should note these caveats in making comparisons to observationally measured GMC lifetimes.

3 RESULTS

3.1 The distribution of GMC lifetimes

We now present our first results on GMC lifetimes via cloud tracking. To increase the number of GMCs in our sample, we stack the results from multiple snapshots in the 100 Myr preceding $z = 0$. To prevent double-counting, we space the reference snapshots to be 10 Myr apart, comparable to the longest GMC lifetimes that we find. Figure 3 shows the distribution of GMC lifetimes. We include only GMCs beyond galactocentric radius of 1 kpc, and we examine only our most resolved clouds, with more than 100 elements. Solid lines show all GMCs, while dashed lines show only those that formed stars during their lifetime. We find a mean lifetime of ~ 6 Myr, with a maximum lifetime of 20 Myr. Table 1 lists these mean lifetimes with their 1-sigma scatter.

3.2 The variation of GMC lifetimes with environment and GMC properties

The distributions of GMC lifetimes in Figure 3 show little galaxy-to-galaxy variation. We now ask how these lifetimes depend on GMC properties and location. Figure 4 shows how GMC lifetimes depend on galactocentric radius (top), fraction of mass in a cloud that is converted to stars during its lifetime (middle), and GMC mass at selection time (bottom), averaged across the 3 simulated galaxies. For the top and bottom panels, we include the full population of resolved GMCs, but in the middle panel we include only the most-resolved population, with $N_p > 100$.

Figure 4 shows that GMC lifetimes increase slightly from the center to the edge of the galaxy, by ~ 2 Myr on average. This is consistent with the trend of the galactic free-fall time with galactocentric radius, which similarly increases by ~ 2 Myr from the inner to outer-most parts of the galaxies. Here, the free-fall time, $t_{ff} = \sqrt{(3/32\pi G\rho)}$, is measured on 100 pc apertures centred on the GMCs. Another key question is what, if any, influence star formation has on GMC lifetimes. Across all of our clouds, 64% form at least

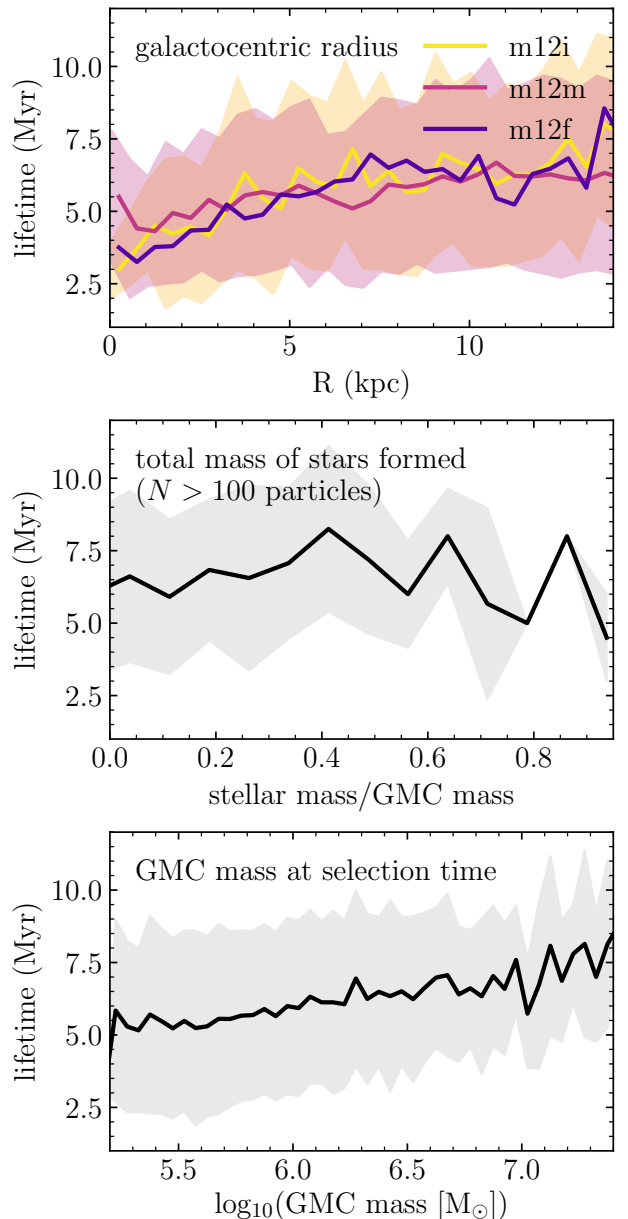


Figure 4. The dependence of GMC lifetime on galactocentric radius (top), mass of stars formed in the GMC (middle), and GMC mass (bottom). In each case, the shaded region denotes the $1 - \sigma$ variation and the black line denotes the mean trend. In the middle panel, we consider only the most resolved clouds, with more than 100 elements. Only for the galactocentric radius do we separate clouds based on their host galaxy, as different galaxies show different environmental variation. We find a slight increase in both the cloud lifetime as a function of radius and as a function of cloud mass, however, little dependence on the amount of star formation

one star particle during their lifetime. As Figure 4 (middle) and Table 1 show, we find no dependence of GMC lifetime on the mass of stars formed over its lifetime. It is intriguing that the amount of star formation appears to play little role in affecting the GMC lifetime. Finally, as Figure 4 (bottom) shows, the lifetime does increase somewhat with GMC

mass. This is consistent with trends seen in other work (e.g. Oklopčić et al. 2017; Hopkins et al. 2012).

In future work, we will use even higher-resolution simulations to pose these question across a larger range of GMC masses, including any differences between GMCs with dispersed star formation versus dense massive clusters.

3.3 Observational methods of determining GMC lifetimes

To make meaningful comparisons to observational inferences of GMC lifetimes, one must understand the methods and assumptions used. In this work, we measure GMC lifetimes via the length of time that gas remains in an identified over-dense structure. Many different definitions of GMC lifetimes have been used, ranging from the emission lifetime of CO to the lifetime of H₂ molecules themselves, and it is important to understand these differences as we make comparisons to observationally determined lifetimes. We will pursue similar observationally based metrics of cloud lifetimes and comparisons of these in future works. However, for context, we review and compare to findings from a selection of other methods.

One approach is to infer lifetimes based on the positions of GMCs along HI filaments. In M33, for example, most GMCs still are associated with their HI filaments, which suggests that they do not live long enough to drift across/off the filament: using this method, Engargiola et al. (2003) infer an upper limit of 10 – 20 Myr on GMC lifetimes.

Another approach is to assume that GMCs go through different evolutionary states and classify them accordingly: this method requires correlating catalogs for GMCs, HII regions, and young stellar objects. Using this methodology inferred multiple studies have inferred that GMC lifetimes are 20 – 40 Myr (e.g. Kawamura et al. 2009; Miura et al. 2012).

Kruijssen & Longmore (2014) and Kruijssen et al. (2018) use a statistical method to measure GMC lifetimes. This is enabled using the uncertainty principle for star formation, which assumes that there is a correlation between GMCs and star-forming regions at different scales. Kruijssen et al. (2019) applied this method to NGC 300, inferring GMC lifetimes of ∼ 10 Myr (Kruijssen et al. 2019).

In summary, observational inferences suggest GMC lifetimes of 10 – 40 Myr. In comparison, our cosmological simulations of MW/M31-like galaxies, which resolve massive GMCs, have mean lifetimes of ∼ 6 Myr and maximum lifetimes of ∼ 20 Myr. While our measurements favour shorter lifetimes, they are broadly consistent with both numerical (e.g. Dobbs & Pringle 2013; Grisdale et al. 2019) and observational studies (see above). It is worth noting that these initial results are sensitive to the method used. Specifically, the mass fraction required for cloud survival plays a large role. Lowering this limit can increase the cloud lifetime by at most a factor of 2.

4 SUMMARY AND CONCLUSIONS

For the first time we have measured the lifetimes of GMCs in cosmological simulations. We find an average lifetime of 5 – 7 Myr, with few clouds surviving past 20 Myr. We find little variation in the distribution of GMC lifetimes across our 3

simulated galaxies (**m12m**, **m12i**, and **m12f**). We find limited dependence of the lifetime on GMC mass, although we can resolve only the most massive clouds, with total gas mass $\gtrsim 10^5 M_\odot$, and we see little dependence on the star formation activity in the cloud. We do find weak dependence of GMC lifetime on galactic environment, with a small increase in the cloud lifetime with increasing galactocentric radius.

The GMC lifetime may be set, in part, by transient compression of gas as it moves through the spiral arms. We plan to explore whether the forcing of structures on timescales shorter than the orbital is contributing to our overall cloud lifetimes. Forthcoming papers will focus on better understanding the connection between GMCs and star formation, including how cloud lifetimes vary as a function of environment and cloud evolutionary history.

ACKNOWLEDGEMENTS

SB, AW, and MB were supported by a Hellman Fellowship, the Heising-Simons Foundation, and NASA, through ATP grant 80NSSC18K1097 and HST grants GO-14734 and AR-15057 from STScI. SRL was supported by NASA through Hubble Fellowship grant #HST-JF2-51395.001-A awarded by STScI. NM was supported by NSERC. PFH was supported by NSF grants 1715847 & 1911233, CAREER grant 1455342, and NASA grants 80NSSC18K0562 & JPL 1589742. DG was supported by the Harlan J. Smith McDonald Observatory Postdoctoral Fellowship. CAFG was supported by NSF grants AST-1517491, AST-1715216, CAREER award AST-1652522, by NASA grant 17-ATP17-0067, by STScI grant HST-GO-14681.011, and by a Cottrell Scholar Award from the Research Corporation for Science Advancement. We ran these simulations and analysis using allocations from: XSEDE AST130039 & AST140064; Blue Waters PRAC NSF.1455342 supported by NSF; and NASA HEC SMD-16-7324, SMD-16-7592, SMD-17-1289, SMD-17-1375, SMD-18-2189.

REFERENCES

- Bland-Hawthorn J., Gerhard O., 2016, *ARA&A*, **54**, 529
- Colombo D., et al., 2014, *ApJ*, **784**, 3
- Dobbs C. L., Pringle J. E., 2013, *MNRAS*, **432**, 653
- Dobbs C. L., Rosolowsky E., Pettitt A. R., Braine J., Corbelli E., Sun J., 2019, *MNRAS*, **485**, 4997
- El-Badry K., et al., 2018a, *MNRAS*, **473**, 1930
- El-Badry K., et al., 2018b, *MNRAS*, **477**, 1536
- Elmegreen B. G., 2007, *ApJ*, **668**, 1064
- Engargiola G., Plambeck R. L., Rosolowsky E., Blitz L., 2003, *ApJS*, **149**, 343
- Faesi C. M., Lada C. J., Forbrich J., 2018, *ApJ*, **857**, 19
- Grisdale K., Agertz O., Renaud F., Romeo A. B., 2018, *MNRAS*, **479**, 3167
- Grisdale K., Agertz O., Renaud F., Romeo A. B., Devriendt J., Slyz A., 2019, *MNRAS*, **486**, 5482
- Grudić M. Y., Hopkins P. F., Faucher-Giguère C.-A., Quataert E., Murray N., Kereš D., 2018, *MNRAS*, **475**, 3511
- Guszejnov D., Grudić M. Y., Offner S. S. R., Boylan-Kolchin M., Faucher-Giguère C.-A., Wetzel A., Benincasa S. M., Loebman S., 2019, arXiv e-prints, p. arXiv:1910.01163
- Harper-Clark E., Murray N., 2011, in Alves J., Elmegreen B. G., Girart J. M., Trimble V., eds, Vol. 270, Computational Star Formation. pp 235–238, doi:10.1017/S1743921311000445

- Hopkins P. F., 2015, *MNRAS*, **450**, 53
 Hopkins P. F., Quataert E., Murray N., 2012, *MNRAS*, **421**, 3488
 Hopkins P. F., et al., 2018, *MNRAS*, **480**, 800
 Howard C. S., Pudritz R. E., Harris W. E., 2017, *MNRAS*, **470**, 3346
 Hung C.-L., et al., 2019, *MNRAS*, **482**, 5125
 Jeffreson S. M. R., Kruijssen J. M. D., 2018, *MNRAS*, **476**, 3688
 Kawamura A., et al., 2009, *ApJS*, **184**, 1
 Kruijssen J. M. D., Longmore S. N., 2014, *MNRAS*, **439**, 3239
 Kruijssen J. M. D., Schruba A., Hygate A. e. P. S., Hu C.-Y.,
 Haydon D. T., Longmore S. N., 2018, *MNRAS*, **479**, 1866
 Kruijssen J. M. D., et al., 2019, *Nature*, **569**, 519
 Krumholz M. R., Gnedin N. Y., 2011, *ApJ*, **729**, 36
 Krumholz M. R., Matzner C. D., McKee C. F., 2006, *ApJ*, **653**, 361
 Leroy A. K., Walter F., Brinks E., Bigiel F., de Blok W. J. G.,
 Madore B., Thornley M. D., 2008, *AJ*, **136**, 2782
 Licquia T. C., Newman J. A., 2015, *ApJ*, **806**, 96
 Lopez L. A., Krumholz M. R., Bolatto A. D., Prochaska J. X.,
 Ramirez-Ruiz E., Castro D., 2014, *ApJ*, **795**, 121
 Miura R. E., et al., 2012, *ApJ*, **761**, 37
 Miville-Deschénes M.-A., Murray N., Lee E. J., 2017, *ApJ*, **834**, 57
 Murray N., 2011, *ApJ*, **729**, 133
 Oklopčić A., Hopkins P. F., Feldmann R., Kereš D., Faucher-
 Giguère C.-A., Murray N., 2017, *MNRAS*, **465**, 952
 Orr M. E., et al., 2018, *MNRAS*, **478**, 3653
 Ostriker E. C., McKee C. F., Leroy A. K., 2010, *ApJ*, **721**, 975
 Pettitt A. R., Egusa F., Dobbs C. L., Tasker E. J., Fujimoto Y.,
 Habe A., 2018, *MNRAS*, **480**, 3356
 Roman-Duval J., Jackson J. M., Heyer M., Rathborne J., Simon
 R., 2010, *ApJ*, **723**, 492
 Sanderson R. E., et al., 2018, arXiv e-prints, p. arXiv:1806.10564
 Schinnerer E., et al., 2013, *ApJ*, **779**, 42
 Schinnerer E., et al., 2019, *The Messenger*, **177**, 36
 Schruba A., Kruijssen J. M. D., Leroy A. K., 2019, arXiv e-prints,
 p. arXiv:1908.04306
 Semenov V. A., Kravtsov A. V., Gnedin N. Y., 2017, *ApJ*, **845**, 133
 Shetty R., Vogel S. N., Ostriker E. C., Teuben P. J., 2007, *ApJ*,
 665, 1138
 Sun J., et al., 2018, *ApJ*, **860**, 172
 Ward R. L., Benincasa S. M., Wadsley J., Sills A., Couchman
 H. M. P., 2016, *MNRAS*, **455**, 920
 Wetzel A. R., Hopkins P. F., Kim J.-h., Faucher-Giguère C.-A.,
 Kereš D., Quataert E., 2016, *ApJ*, **827**, L23

This paper has been typeset from a *T*_E*X*/*L*_A*T*_E*X* file prepared by the author.